Supplementary Information (SI) for Journal of Materials Chemistry A.
This journal is © The Royal Society of Chemistry 2025

Supporting Information for

Interface Engineering of 0D-2D Bimetallic $CoSe_2$/ZnSe@MX Heterostructured Electrodes for High-Performance Lithium-Ion Batteries

Fayun Wei[a,b,#], Fanghua Liang[a,#], Yanrui Zhao[a], Zhuyu Ji[a], Tingting Yan[a,*], Ruiqing Li[a], Hui Liu[a,*], Youchao Kong[c], Honggang He[a], Weichuan Huang[d], Chunyan Cao[a,e], Wei Zhang[a], Bin Fei[e,*], Mingzheng Ge[a,*]

[a]School of Textile and Clothing, Nantong University, Nantong 226019, P. R. China

[b]College of Textile Science and Engineering, Zhejiang Sci-Tech University, Hangzhou 310018, P. R. China

[c]Department of Physics and Electronic Engineering, Yancheng Teachers University, Yancheng 224002, P. R. China

[d]School of Chemistry and Chemical Engineering, Nantong University, Nantong 226019, P. R. China

[e]School of Fashion and Textiles, The Hong Kong Polytechnic University, Hong Kong 999077, P. R. China

[#]These authors contributed equally.

1. Supporting Notes

1.1 Lithium ionic conductivity determined by galvanostatic intermittent titration technique (GITT).

1.2 Theoretical analysis of Li-ions adsorption behavior in the electrode.

2. Supporting Figures

Figure S1. SEM image of CoZn-MOFs@MX.

Figure S2. HADDF-STEM image of $CoSe_2$/ZnSe@MX.

Figure S3. XRD image of MAX and MX.

Figure S4. High-resolution XPS spectra of a) Ti 2p, b) C 1s, c) N 1s and d) O 1s of $CoSe_2$/ZnSe@MX.

Figure S5. CV curves of $CoSe_2$/ZnSe@MX electrode at different scan rates from 0.1 to 5 mV s^{-1}.

Figure S6. a) GITT profile for $CoSe_2$/ZnSe@MX and $CoSe_2$/ZnSe during charge/discharge process. b) GITT profile of a single titration for $CoSe_2$/ZnSe@MX during discharging process.

Figure S7. Initial 5 charge/discharge profiles of $CoSe_2$/ZnSe@MX and $CoSe_2$/ZnSe electrode at 0.1 A g^{-1}.

Figure S8. Long cycling performance of MX.

Figure S9. a) Low and b) high resolution HRTEM image of $CoSe_2$/ZnSe@MX after long cycling.

Figure S10. Initial 5 charge/discharge profiles of $CoSe_2$/ZnSe@MX//LFP at 0.1 A g^{-1}.

Figure S11. Long cycling performances of $CoSe_2$/ZnSe@MX//LFP full cell.

3. Supporting Tables

Table S1. The EIS fitting results of $CoSe_2$/ZnSe@MX, $CoSe_2$/ZnSe and MX.

Table S2. Comparison of performance in this work to the previously published literatures on transition metal selenide-based anodes.

1. Supporting Notes

1.1 Lithium ionic conductivity determined by galvanostatic intermittent titration technique (GITT)

To further study the lithium-ion diffusion performance of $CoSe_2$/ZnSe@MX composite electrode at low current density, the lithium-ion diffusion coefficient was calculated by constant current intermittent titration technique (GITT). Before performing GITT measurements, the electrode was activated at 0.1 A g^{-1} to obtain a stable SEI film. The lithium-ion diffusivity (D_{Li^+}) could be calculated by the quotation as following:

$$D = \frac{4}{\pi t}\left(\frac{n_m V_m}{S}\right)^2\left(\frac{\Delta E_s}{\Delta E_t}\right)^2$$

Where t is the time of the current pulse, n_m is the number of moles, V_m is the molar volume of the electrode, and S is the contact area between the active material and the electrolyte. ΔE_S and ΔE_t respectively represent the steady-state voltage change that occurs through the current pulse and the voltage difference before and after the current pulse.[1] In this GITT teat, the battery was discharged/charged between at 0.1 A g^{-1}, and then relaxed under open circuit for 900s (Figure S6).

1.2 Theoretical analysis of Li-ions adsorption behavior in the electrode.

We have employed the Vienna Ab Initio Package (VASP) to perform all density functional theory (DFT) calculations within the generalized gradient approximation (GGA) using the PBE formulation.[2-4] We have chosen the projected augmented wave (PAW) potentials to describe the ionic cores and take valence electrons into account

using a plane wave basis set with a kinetic energy cutoff of 450 eV.[5, 6] Partial occupancies of the Kohn-Sham orbitals were allowed using the Gaussian smearing method and a width of 0.05 eV. The electronic energy was considered self-consistent when the energy change was smaller than 10^{-5} and 10^{-6} eV for structure optimization and DOS calculation, respectively. A geometry optimization was considered convergent when the force change was smaller than 0.02 eV/Å. Grimme's DFT-D3 methodology was used to describe the dispersion interactions. The Brillouin zone integral uses the surfaces structures of Monkhorst-Pack K point sampling (3×3×1) for the structure optimization and electron calculation.[7] The adsorption energy is calculated as,

$$E_{ads} = E(\text{slab+Li})-E(\text{slab})-E(\text{Li})$$

Where E_{ads} is the adsorption energy. E(slab+M) is the energy of the system with one Li atom on the surface slab. E(slab) is the energy of the surface slab without the adsorbate. E(M) is the energy of the isolated Li, which is -1.91 eV.

2. Supporting Figures

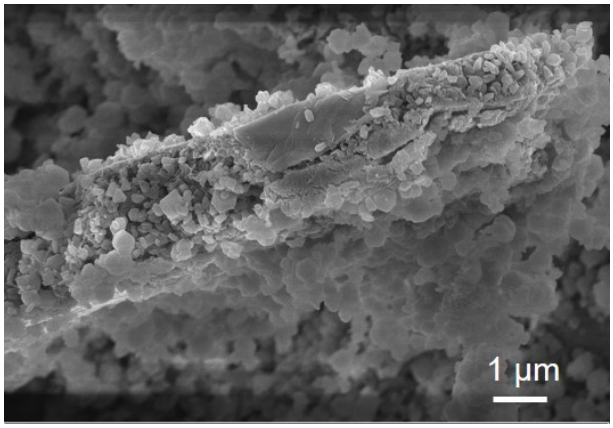

Figure S1. SEM image of CoZn-MOFs@MX.

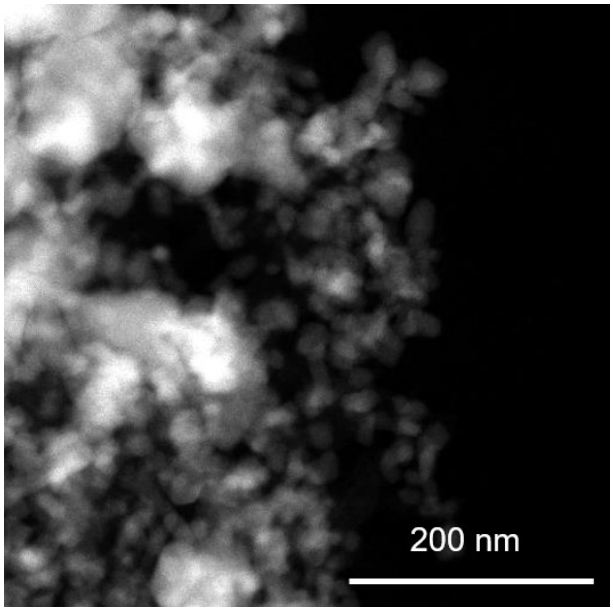

Figure S2. HADDF-STEM image of $CoSe_2$/ZnSe@MX.

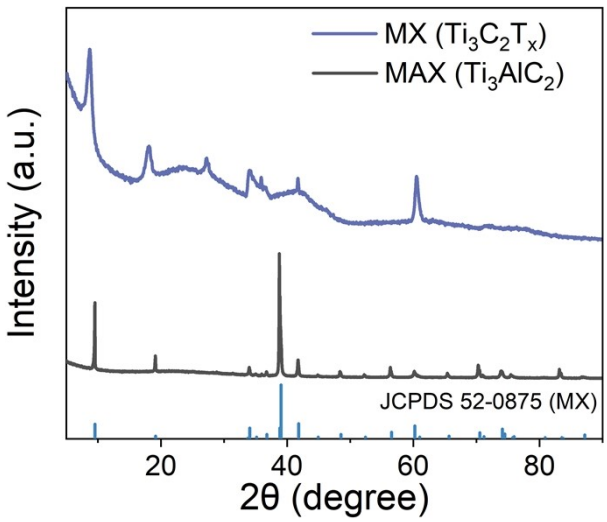

Figure S3. XRD image of MAX and MX.

Discussion: Figure S3 shows a prominent characteristic peak at 39°, corresponding to the (104) lattice plane. Compared to Ti_3AlC_2 MAX, the absence of the (104) peak in $Ti_3C_2T_x$ MX confirms the successful etching of the "Al" layers. Additionally, the diffraction peak for the (002) crystal plane shifts from 9.5° to 8.8°, further supporting the synthesis of $Ti_3C_2T_x$ MX.

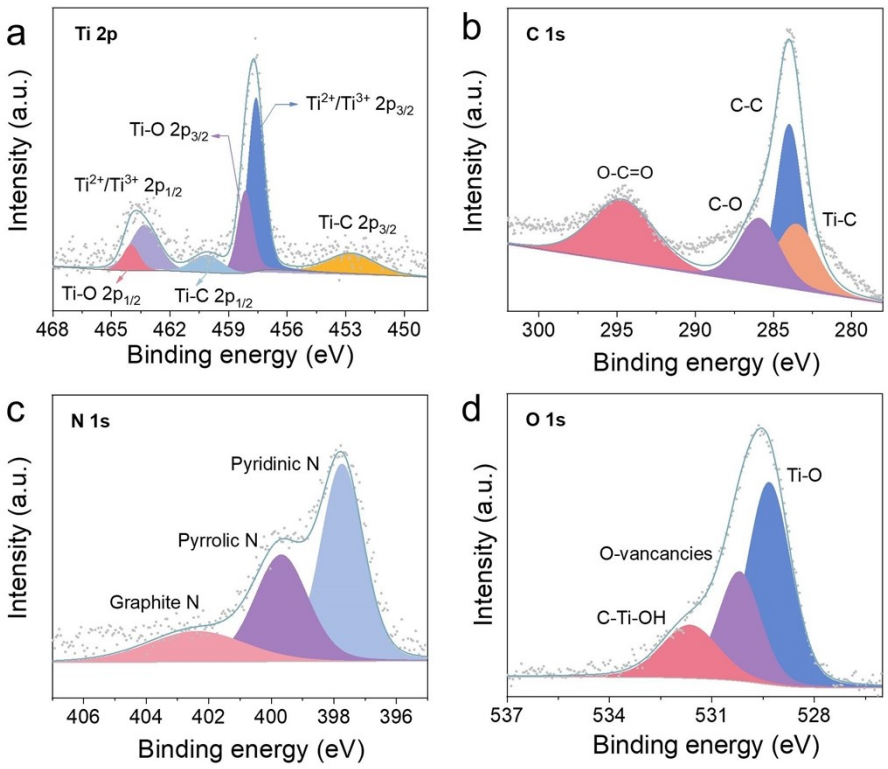

Figure S4. High-resolution XPS spectra of a) Ti 2p, b) C 1s, c) N 1s and d) O 1s of $CoSe_2$/ZnSe@MX.

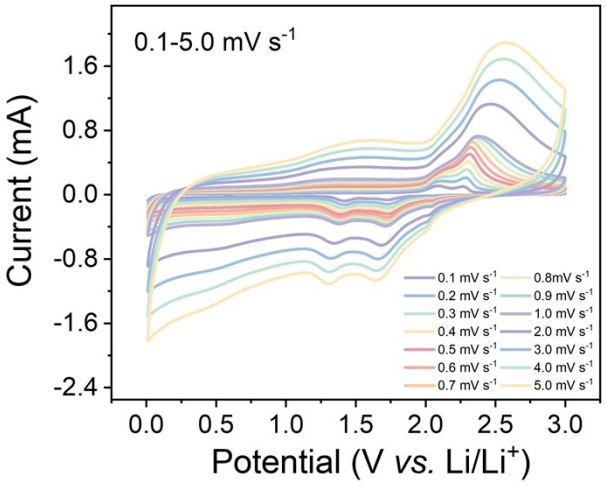

Figure S5. CV curves of $CoSe_2$/ZnSe@MX electrode at different scan rates from 0.1 to 5 mV s^{-1}.

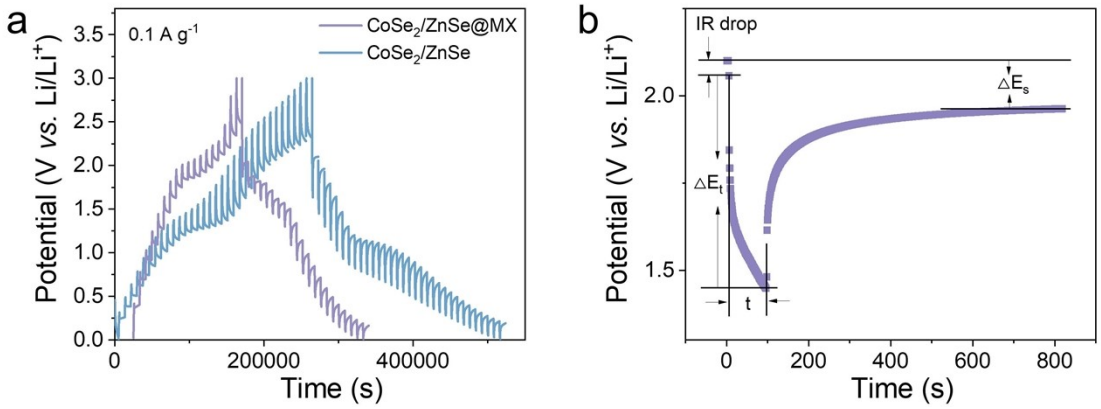

Figure S6. a) GITT profile for $CoSe_2$/ZnSe@MX and $CoSe_2$/ZnSe during charge/discharge process. b) GITT profile of a single titration for $CoSe_2$/ZnSe@MX during discharging process.

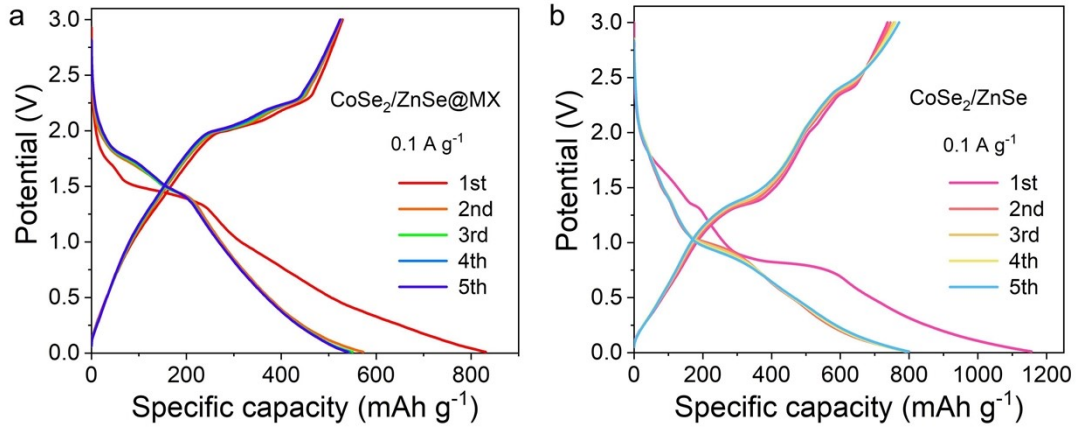

Figure S7. Initial 5 charge/discharge profiles of $CoSe_2$/ZnSe@MX and $CoSe_2$/ZnSe electrode at 0.1 A g^{-1}.

Discussion: The initial charge/discharge specific capacity of $CoSe_2$/ZnSe is 737.3, 1156 mAh g^{-1} at 0.1 A g^{-1}, with an initial columbic efficiency (ICE) of 63.7%, which owing to the lack of MX with high conductivity as a stabilizing support.

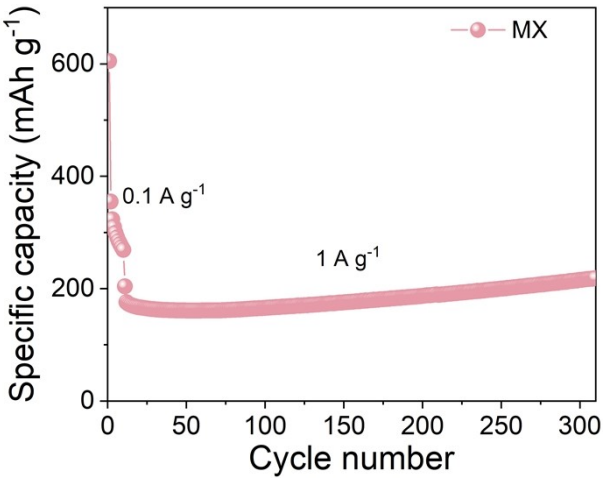

Figure S8. Long cycling performance of MX.

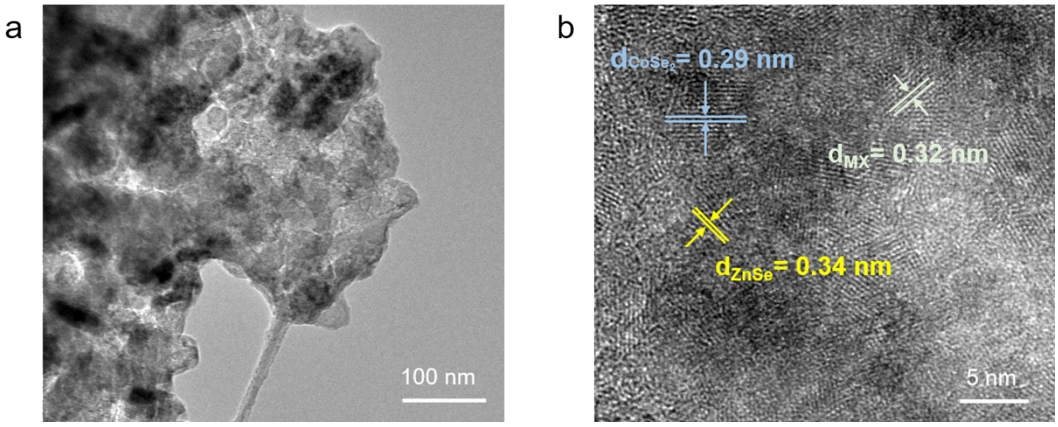

Figure S9. a) Low and b) high resolution HRTEM image of $CoSe_2$/ZnSe@MX after long cycling.

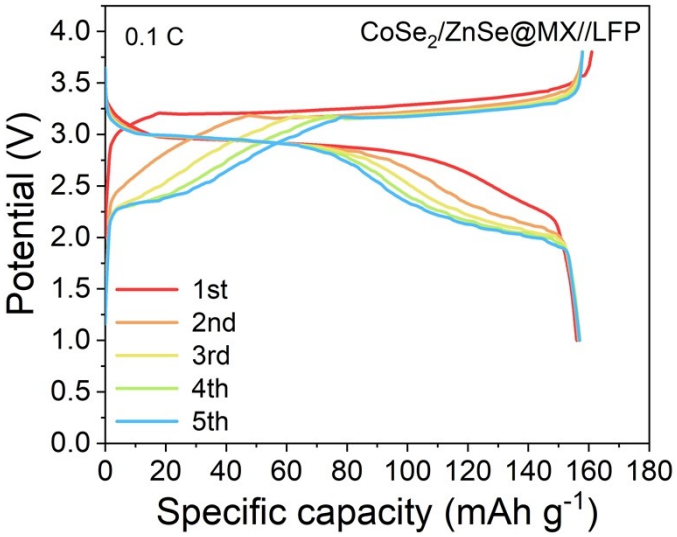

Figure S10. Initial 5 charge/discharge profiles of $CoSe_2$/ZnSe@MX//LFP at 0.1 A g^{-1}.

Discussion: The initial charge/discharge specific capacity of $CoSe_2$/ZnSe@MX//LFP full cell is 160.9, 156 mAh g^{-1}, with an ICE of 96.9% and a charge/discharge plateau of 3.21V and 2.94 V, respectively.

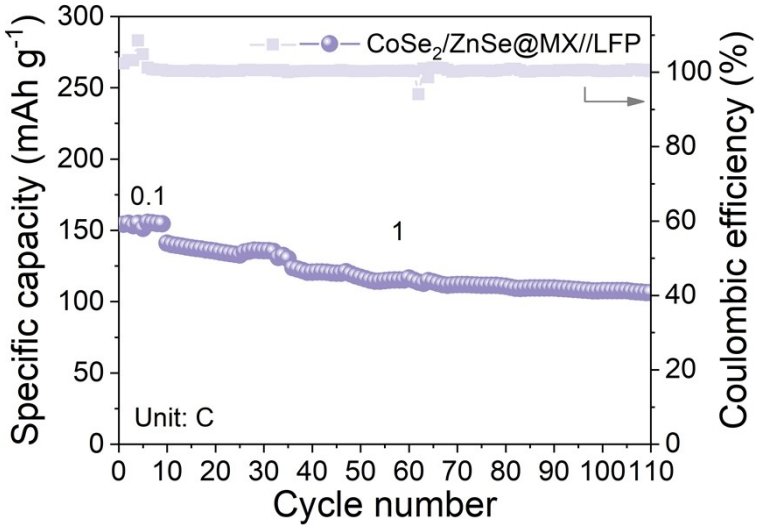

Figure S11. Long cycling performances of $CoSe_2$/ZnSe@MX//LFP full cell.

3. Supporting Tables

Table S1. The EIS fitting results of $CoSe_2$/ZnSe@MX, $CoSe_2$/ZnSe and MX.

Material	R_s/Ω	R_{ct}/Ω
$CoSe_2$/ZnSe@MX	1.62	77.6
$CoSe_2$/ZnSe	13.4	88.8
MX	28.9	132.3

Table S2. Comparison of performance in this work to the previously published literatures on transition metal selenide-based anodes.

Anode	Current density (A g^{-1})	Cycle number	Discharge capacity (mAh g^{-1})	Ref.
$CoSe_2$ HBs/$Ti_3C_2T_x$	0.5	3000	186.8	[8]
$CoSe_2$@C	0.05	100	691	[9]
$CoSe_2$@N-CF/CNTs	1	500	428	[10]
ZnSe/$CoSe_2$-C	1	500	700	[11]
ZnSe/CoSe/NC	1	500	624.6	[12]
ZnSe@N-CNFs	2	200	365.6	[13]
N-ZnSe@rGO	2	1000	464	[14]
ZnSe/CeO_2/RGO	0.3	250	534.8	[15]
Cu-doped $CoSe_2$	1	200	807	[16]
$CoSe_2$@CNWs	2	500	300	[17]
ZnSe@$CoSe_2$	1	500	615	[18]
Nb_2CT_x MXene	0.5	1500	288	[19]
$Ti_3C_2T_x$@$MoSe_2$	0.3	800	230	[20]
P-Ti_3C_2	1	2000	~100	[21]
Ni(OH)$_2$/d-Ti_3C_2	1	1000	372	[22]
P-$CoSe_2$@NGC	2	2000	~150	[23]
$CoSe_2$/ZnSe@MX	**1** **1** **1**	**300** **1000** **2000**	**728.2** **536.7** **293.9**	**This work**

Reference

1. C. Cao, H. Dong, F. Liang, Y. Zhang, W. Zhang, H. Wang, H. Shao, H. Liu, K. Dong, Y. Tang, Y. Lai and M. Ge, *Chem. Eng. J.*, 2021, **416**, 129094.
2. G. Kresse and D. Joubert, *Phys. Rev. B*, 1999, **59**, 1758-1775.
3. J. P. Perdew, K. Burke and M. Ernzerhof, *Phys. Rev. Lett.*, 1996, **77**, 3865-3868.
4. G. Kresse and J. Furthmuller, *Phys. Rev. B*, 1996, **54**, 11169-11186.
5. S. Grimme, S. Antony J Fau - Ehrlich, H. Ehrlich S Fau - Krieg and H. Krieg.
6. P. E. Blöchl, *Physical Review B*, 1994, **50**, 17953-17979.
7. G. Henkelman, B. P. Uberuaga and H. Jónsson, *J. Chem. Phys.*, 2000, **113**, 9901-9904.
8. L. Zhang, W. Liu, Q. Ma, Y. Xu, Z. Liu and G. Wang, *ChemElectroChem*, 2021, **8**, 4047-4053.
9. N. Yu, L. Zou, C. Li and K. Guo, *Appl. Surf. Sci.*, 2019, **483**, 85-90.
10. J. Yang, H. Gao, S. Men, Z. Shi, Z. Lin, X. Kang and S. Chen, *Adv. Sci.*, 2018, **5**, 1800763.
11. K. Wang, Y. P. Wang, Y. F. Zhang, F. Liu, J. R. Shi, S. Y. Liu, X. F. Xie, G. Z. Cao and A. Q. Pan, *Nanoscale*, 2020, **12**, 12623-12631.
12. H. Liu, Y. Lin, M. Li, L. Zhang, Y. Lu and W. Xiao, *Int. J. Hydrogen Energy*, 2021, **46**, 30818-30827.
13. P. Zhou, M. Y. Zhang, L. P. Wang, Q. Z. Huang, Z. A. Su, L. W. Li, X. D. Wang, Y. H. Li, C. Zeng and Z. H. Guo, *Front. Chem.*, 2019, **7,** 569.
14. X. B. Liu, Y. C. Liu, M. Feng and L. Z. Fan, *J. Mater. Chem. A*, 2018, **6**, 23621-23627.
15. C. Dong, Y. Zhou, W. Liu, W. Du, X. Zhang, X. Sun, L. Kang, X. Zhang and F. Jiang, *J. Alloys Compd.*, 2021, **875**, 159903.
16. D. Chen, G. Chen, J. Pei, Y. Hu, Z. Qin, J. Wang and F. Wu, *ChemElectroChem*, 2017, **4**, 2158-2163.
17. Q. Xiao, Q. Song, K. Zheng, L. Zheng, Y. Zhu and Z. Chen, *Nano Energy*, 2022, **98**, 107326.
18. Y. M. Lin, H. S. Fan, C.-Z. Zhu and J. Xu, *Rare Metals*, 2022, **41**, 4104-4115.
19. R. Liu, W. Cao, D. Han, Y. Mo, H. Zeng, H. Yang and W. Li, *J. Alloys Compd.*, 2019, **793**, 505-511.
20. J. Zhong, L. Qin, J. Li, Z. Yang, K. Yang and M. Zhang, *Int. J Min. Met. Mater.,* 2022, **29**, 1061-1072.
21. N. Xue, X. Li, M. Zhang, L. Han, Y. Liu and X. Tao, *ACS Appl. Energy Mater.*, 2020, **3**, 10234-10241.
22. C. Li, Z. Xue, J. Qin, M. Sawangphruk, P. Yu, X. Zhang and R. Liu, *J. Alloys Compd.*, 2020, **842**, 155812.
23. J. S. Lee, R. Saroha and J. S. Cho, *Nano-Micro Lett.*, 2022, **14**, 113.